

See discussions, stats, and author profiles for this publication at: <https://www.researchgate.net/publication/7015932>

# Polyelectrolyte Films Based on Polysaccharides of Different Conformations: Effects on Multilayer Structure and Mechanical Properties

ARTICLE in BIOMACROMOLECULES · JULY 2006

Impact Factor: 5.75 · DOI: 10.1021/bm060378a · Source: PubMed

CITATIONS

54

READS

82

6 AUTHORS, INCLUDING:



Nicolas Delorme

Université du Maine

54 PUBLICATIONS 593 CITATIONS

SEE PROFILE



Gleb Sukhorukov

Queen Mary, University of London

318 PUBLICATIONS 19,269 CITATIONS

SEE PROFILE



Andreas Fery

Leibniz Institute of Polymer Research Dresden

251 PUBLICATIONS 4,822 CITATIONS

SEE PROFILE



Karine Glinel

Université catholique de Louvain

55 PUBLICATIONS 1,795 CITATIONS

SEE PROFILE

# Polyelectrolyte Films Based on Polysaccharides of Different Conformations: Effects on Multilayer Structure and Mechanical Properties

Bjoern Schoeler,<sup>†</sup> Nicolas Delorme,<sup>‡</sup> Ingo Doench,<sup>‡</sup> Gleb B. Sukhorukov,<sup>‡,§</sup>  
Andreas Fery,<sup>‡</sup> and Karine Glinel<sup>\*,†</sup>

UMR 6522, Polymères, Biopolymères, Membranes, CNRS - Université de Rouen, Bd Maurice de Broglie,  
F-76821 Mont-Saint-Aignan, France, and Max Planck Institute of Colloids and Interfaces, Am Mühlenberg,  
D-14424 Potsdam, Germany

Received April 18, 2006

Ultrathin films were prepared with cationic poly(allylamine hydrochloride) (PAH) and two anionic polysaccharides, *ι*- and *λ*-carrageenan, of similar chemical composition but different conformations using the layer-by-layer (LbL) technique. The study of aqueous solutions of carrageenans confirms that *ι*-carrageenan is at room temperature in helical conformation while *λ*-carrageenan is in random coil conformation. Characterization of the multilayers by ellipsometry, circular dichroism, and AFM revealed that *ι*-carrageenan keeps its helical conformation within the films while *λ*-carrageenan chains are in random coil conformation. Investigation of the mechanical properties of the films by performing nanoindentation experiments using force spectroscopy showed clear differences between the two films based on carrageenans of different conformations.

## Introduction

Fabrication of multilayer films by alternatively adsorbing polyelectrolytes of opposite charge has become a powerful method enabling the controlled construction of ultrathin films.<sup>1–4</sup> Of major interest is the possibility to control the vertical structure and thickness of the assemblies in the nanometer range, with lateral control over their size being also achievable in the micrometer<sup>5,6</sup> and nanometer ranges.<sup>7,8</sup> This layer-by-layer (LbL) technique has been used for preparation of functional films for applications in various domains such as biosensing, catalysis, separation membranes, antireflection coatings, optical devices, and drug delivery capsules.<sup>9–13</sup>

An important advantage of polyelectrolyte multilayers is the possibility to tune their internal structure to obtain films with desired properties such as film stability, density, morphology, or porosity. The control of the mechanical properties of the films at the nanometer scale is also of particular interest for many applications in biology or materials science. For example, it was recently shown that the adhesion of biological cells on a coating depends on its mechanical properties.<sup>14–16</sup> Various approaches which consist of changing the charge density of polyelectrolytes,<sup>17</sup> incorporating inorganic particles,<sup>18</sup> carbon nanotubes,<sup>19</sup> or cross-links between polyelectrolyte chains,<sup>14</sup> were tested to change the mechanical properties of LbL films. However, a systematic study of the influence of the polyelectrolyte structure on the mechanical properties of LbL film is still lacking.

In this context, the use of charged polysaccharides which exhibit a large variety of structures and functionality is attractive. Indeed, these biopolymers allow one to get access to a range of

properties, with only very limited variations of the chemical nature of the chains. In addition, they are useful for pharmaceutical or biomedical applications, due to their nontoxicity, biocompatibility, and biodegradability. Among these polysaccharides, carrageenans, which are anionic sulfated polysaccharides extracted from red seaweeds, have found widespread application in food, pharmaceutical, and cosmetic industries, due to their nontoxicity and their gel-forming and viscosifying properties in aqueous solution.<sup>20–22</sup> These polyelectrolytes possess a linear galactan backbone composed of alternating 3-linked  $\beta$ -D-galactopyranose and 4-linked  $\alpha$ -D-galactopyranose or 4-linked 3,6-anhydrogalactose.<sup>21,22</sup> Different types of carrageenans are distinguished depending on the position and the number of sulfate groups on the polysaccharide backbone. In the present work, we used two different carrageenans named *λ* and *ι* (Figure 1), which mainly differ by their conformation in solution.<sup>23</sup> The inspection of the chemical structures of *ι*- and *λ*-carrageenan reveal only slight differences: The sulfate contents of *ι*- and *λ*-carrageenan are 37% and 42% (w/w), respectively; more importantly, *ι*-carrageenan contains 3,6-anhydro bridges. Though small, these structural variations result in very different behaviors in aqueous solution. *λ*-Carrageenan is always present in a random coil conformation and cannot form gels,<sup>22</sup> whereas *ι*-carrageenan adopts a structured helical conformation at room temperature,<sup>22–29</sup> which confers a high viscosity to its water solution. There is still an ongoing debate in the literature about the exact structure of *ι*-carrageenan solutions, whether helices associate in dimers or not.<sup>30–32</sup> This is of minor importance for the present study. Indeed, *ι*- and *λ*-carrageenan strongly differ in chain rigidity and persistence length. For instance, at 0.1 M NaCl, the persistence lengths of *ι*- and *λ*-carrageenan are about 74 and 13 nm, respectively.<sup>25,33</sup> Such a difference is expected to translate to different mechanical properties of their LbL films, a point which we will explore here. Indeed, no study was reported so far on LbL grown from chains of close chemical composition and charge density, only

\* Author for correspondence. E-mail: karine.glinel@univ-rouen.fr. Phone: ++ 33 2 35 14 65 86. Fax: ++ 33 2 35 14 67 04.

<sup>†</sup> CNRS - Université de Rouen.

<sup>‡</sup> Max Planck Institute of Colloids and Interfaces.

<sup>§</sup> Present address: Department of Materials, Mile End Road, Queen Mary, University of London, E1 4NS, United Kingdom.

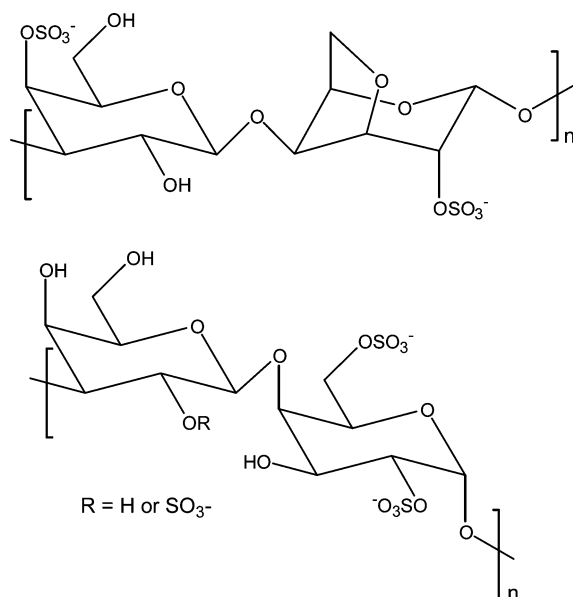


**Figure 1.** Schematic representation of the repeating disaccharide units of  $\iota$ -carrageenan (top) and  $\lambda$ -carrageenan (bottom).

differing in their solution conformation. This knowledge would allow one to fine-tune the physical properties of LbL assemblies, while keeping essentially identical chemical properties. In addition,  $\iota$ -carrageenan possesses a thermosensitive behavior,<sup>22,34</sup> displaying a reversible helix–random coil conformational transition upon heating. The transition temperature depends on concentration of the polysaccharide and ionic strength.<sup>34,35</sup> Such a thermosensitive behavior is also of potential interest to develop stimuli-responsive materials as previously demonstrated for synthetic poly(*N*-isopropylacrylamide) (PNIPAM) derivatives.<sup>36,37</sup>

In this paper, we study LbL films prepared with weakly charged poly(allylamine hydrochloride) (PAH) and these two carrageenans. Our motivation is to investigate the influence of the conformation of both polysaccharides in solution on the films characteristics such as thickness, surface morphology, microstructure, and mechanical properties. We show that the slight chemical difference between these two types of chains, which translates into different solution properties and multilayered structures, strongly affects the characteristics of the LbL films, especially their mechanical properties.

## Experimental Section

**Material.** Poly(ethyleneimine) (PEI) ( $M_w = 750\,000\text{ g}\cdot\text{mol}^{-1}$ ), poly(allylamine hydrochloride) (PAH) ( $M_w = 70\,000\text{ g}\cdot\text{mol}^{-1}$ ) ( $pK_a \approx 8.5$ ), and 3-aminopropyl triethoxysilane (APTES) were purchased from Sigma-Aldrich. Purified  $\iota$ -carrageenan (Gelcarin) and  $\lambda$ -carrageenan (Viscarin GP-109) (Figure 1) were gifts from FMC Corporation (Belgium). Potassium chloride (KCl) was supplied by Merck. All chemicals and polyelectrolytes were used without any further purification.

**Solutions of Polyelectrolytes.** The solution of  $\iota$ -carrageenan was prepared at a concentration of  $3\text{ g}\cdot\text{L}^{-1}$  by adding the polysaccharide in small portions in pure Milli-Q water at  $T = 40\text{ }^\circ\text{C}$  under mechanical stirring for 1 h. The solution was heated to  $80\text{ }^\circ\text{C}$  and stirred for 30 min, then cooled at room temperature to obtain a clear and homogeneous solution of  $\iota$ -carrageenan. The water evaporation was prevented during the heating by using a water-jacketed condenser. The solutions of PEI, PAH, and  $\lambda$ -carrageenan were prepared at room temperature by dissolving the polymers in pure Milli-Q water (resistivity  $> 18\text{ M}\Omega$ ) at a concentration of  $3\text{ g}\cdot\text{L}^{-1}$ . The ionic strength of the carrageenan

solutions was adjusted to  $0.01\text{ M}$  KCl, to limit the viscosity of the solution and avoid aggregation. By contrast, the ionic strength of the PAH solution was increased to  $0.1\text{ M}$  KCl, to ensure a larger thickness increment. The pH of PAH and carrageenan solutions was set to 7 or 10 by adding  $0.1\text{ M}$  KOH. All solutions were filtered through a  $8\text{ }\mu\text{m}$  Millipore membrane before use.

**Multilayer Film Preparation.** Multilayer films were prepared on one-side polished (100) silicon wafers cut into  $3\text{ cm}$  by  $1\text{ cm}$  rectangles (Silchem Handelsgesellschaft mbH, Germany) or SUPRASIL-type fused silica plates (Hellma, France). The substrates were first cleaned by treatment in a hot piranha solution ( $\text{H}_2\text{O}_2$  (35%): $\text{H}_2\text{SO}_4$  (98%) 1:1 v/v) (caution: piranha solution is extremely corrosive) for at least 20 min followed by intense rinsing with pure Milli-Q water. The cleaned substrates were dipped at the first step for 20 min in the PEI solution. Then, anionic carrageenan and cationic PAH were alternatively adsorbed by dipping the samples in polyelectrolyte solutions. After each adsorption step, the samples were rinsed by dipping in three different beakers of an aqueous solution adjusted to the same pH ( $\pm 0.1$ ) as the adsorption solutions by addition of  $0.1\text{ M}$  KOH. A dipping robot (Riegler Kirstein GmbH, Germany) was used to prepare very thick multilayers. The samples were post-assembly dried with a stream of pure air before analysis. A film prepared with  $N - 1$  layers of PAH and  $N$  layers of carrageenan will be named (PAH/carr) $_N$  in the following.

**Experimental Techniques. Ellipsometry.** The thickness of the multilayers grown on silicon wafers was determined by a null ellipsometer from Multiskop Ellipsometer (Optrel GbR, Germany) at a fixed angle of  $70^\circ$  and a fixed wavelength of  $632.8\text{ nm}$ . The refractive indexes of the silicon and the polyelectrolyte films were taken to be  $3.882 - j0.019$  and  $1.51$ , respectively. For each sample, at least five spots were measured and averaged. The thickness of the native oxide layer atop the silicon substrate ( $\sim 15\text{ \AA}$ ) was systematically subtracted from the computed total film thickness.

**Polarimetry.** The observed optical rotation ( $\alpha$ ) of carrageenan solutions was monitored at  $546\text{ nm}$  (Hg lamp) as a function of the temperature with a Perkin-Elmer 241 polarimeter equipped with a  $10\text{ cm}$  jacketed cell and a circulating water bath for accurate temperature control. Care was taken to allow the temperature equilibrium between each measurement.

**Circular Dichroism.** Circular dichroism (CD) measurements were carried out at room temperature with a CD6 dichrograph (Jobin-Yvon, France). The measuring chamber was extensively purged with pure nitrogen gas before the measurement to remove any trace of oxygen perturbing the CD spectra. Scans were performed at a rate of  $0.1\text{ nm}\cdot\text{s}^{-1}$  with a sampling interval of  $0.5\text{ nm}$  from  $180$  to  $192\text{ nm}$  and at a rate of  $0.33\text{ nm}\cdot\text{s}^{-1}$  from  $190$  to  $220\text{ nm}$  with a sampling interval of  $1\text{ nm}$ . For each measurement, four spectra were recorded and averaged to improve the signal/noise ratio. The fused silica slides coated by the multilayers were mounted in a dedicated sample holder. In the case of carrageenan solutions, a quartz cell with a optical path length of  $0.1\text{ cm}$  was used. The CD spectra of the films and the carrageenan solutions were systematically corrected by the spectra corresponding to uncoated fused silica slide and buffer solution, respectively.

**Atomic Force Microscopy.** All AFM images and force measurement curves were recorded with a NanoWizard AFM (JPK instrument, Berlin).

**Imaging.** Images were recorded in intermittent-contact mode using a silicon tip (Nanoworld – Arrow NCR) with a nominal spring constant of  $42\text{ N}\cdot\text{m}^{-1}$ . For imaging in liquid, Milli-Q water adjusted to the pH of the assembly solutions (pH 10) was used. Roughness measurements were all performed by using the same tip, the same scan rate ( $1\text{ Hz}$ ), and two different scan sizes ( $8 \times 8$  and  $4 \times 4\text{ }\mu\text{m}^2$ ). Thicknesses of the films in aqueous solution were determined by scratching off a part of the film followed by scanning over the film edge region.

**AFM Force Measurements.** The mechanical properties of the samples were investigated by measuring force vs distance curves. These experiments were performed on thick films ( $> 200\text{ nm}$ ), and the indentation depths used did not exceed 10% of the film thickness in

order to avoid any undesirable artifacts due to the large stiffness of the substrate.<sup>38</sup> We used a contact-mode cantilever (Ultrasharp – CSC12/AIBS) with a spring constant  $k$  measured by two independent methods: the thermal-oscillation method<sup>39</sup> and the Sader's method<sup>40</sup> leading to a typical error of 10%.<sup>41</sup> The spring constant  $k = 417 \text{ pN}\cdot\text{nm}^{-1}$  corresponds to the average of the values obtained by these two methods. To reduce adhesion between the substrate and the tip, the cantilever was modified by aminosilane. For this, we used a silanization procedure consisting of dipping the commercial cantilever into a 10% solution of APTES in toluene for 1 h.<sup>42</sup> The cantilever is then washed several times with fresh toluene. The tip radius ( $R$ ) measured after the surface modification by blind reconstruction of the tip geometry<sup>43</sup> was estimated to be 50 nm.

The force–distance curves were analyzed using the PUNIAS software developed by P. Carl and P. Dalhaimer.<sup>44</sup> To determine the Young's modulus, the approach curve was fitted by using several models based on the Hertz sphere model.<sup>45</sup> According to these models, the relation between the Young's modulus ( $E$ ), the force ( $F$ ), and the deformation ( $\delta$ ) is

$$F = \frac{4}{3(1-\nu^2)} \times ER^{1/2}\delta^{3/2} + f(h) \quad (1)$$

where  $R$  is the radius of the sphere tip (50 nm),  $\nu$  is the Poisson ratio, and  $f(h)$  is a correction term depending on the film thickness. For polymeric systems, the Poisson ratio is between 0.33 and 0.5 for polymer and incompressible materials, respectively. Considering the nature of the studied materials and since no independent measurement allows the determination of the exact Poisson ratio, we chose a value of 0.33 for  $\nu$ .<sup>46</sup> Anyway, the role of the Poisson ratio is transparent, allowing the reader to follow the effect of it on the Young's modulus value, which is rather minor for the expected range of Poisson ratio for polymeric material between 0.33 and 0.5.

## Results and Discussion

In contrast to  $\lambda$ -carrageenan, which always takes a random coil conformation in aqueous solution (since its persistence length of about  $13 \text{ nm}$ <sup>33</sup> is well below the extended chain length), the conformation of  $\iota$ -carrageenan strongly depends on the ionic strength and the temperature of the solution.<sup>22,24–29</sup> For this reason, we first checked macromolecular conformations of  $\iota$ - and  $\lambda$ -carrageenan in aqueous solution at neutral pH by circular dichroism and polarimetry. These studies were performed in the presence of 0.01 M KCl, which is known to induce a helix conformation of  $\iota$ -carrageenan chains.<sup>35</sup> In addition, the polysaccharides were solubilized at low concentration ( $3 \text{ g}\cdot\text{L}^{-1}$ ) to prevent the formation of viscous solutions. Figure 2 displays the CD spectra of dilute solutions of  $\iota$ - and  $\lambda$ -carrageenan recorded at room temperature from 180 to 220 nm. Whereas no band is detected on the spectrum of the  $\lambda$ -carrageenan, a clear decrease of the dichroic signal is observed at wavelengths below 195 nm for  $\iota$ -carrageenan. Previous measurements performed by others<sup>27</sup> with a vacuum ultraviolet CD spectrometer working between 150 and 200 nm revealed that the spectrum of  $\iota$ -carrageenan measured at room temperature exhibits a negative and a positive band positioned at 180 and 165 nm, respectively, due to the presence of the helical structure. Since recording spectrum below 180 nm is difficult due to technical reasons, the observed decrease of the dichroic signal observed below 195 nm is in agreement with the presence of the negative band centered at 180 nm previously observed.<sup>27</sup> In addition, polarimetry measurements performed at room temperature (Figure 3) reveal that the  $\iota$ -carrageenan solution exhibits a higher rotation ( $\alpha$ ) than the  $\lambda$ -carrageenan solution. These different results confirm that  $\lambda$ -carrageenan macromol-

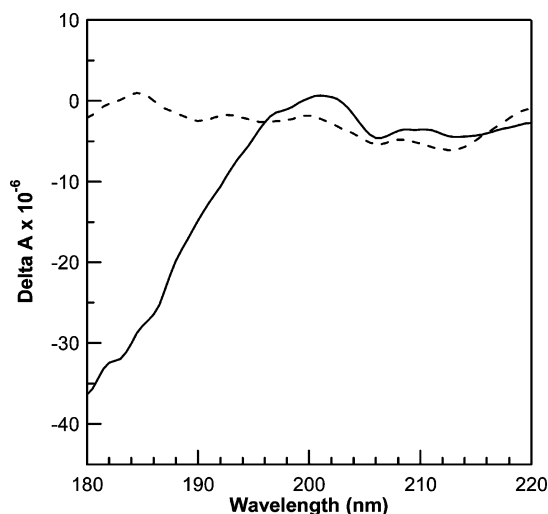


**Figure 2.** Circular dichroism spectra of  $\lambda$ -carrageenan (dashed line) and  $\iota$ -carrageenan (continuous line) solutions ( $3 \text{ g}\cdot\text{L}^{-1}$  in 0.01 M KCl, pH 7) measured at room temperature.

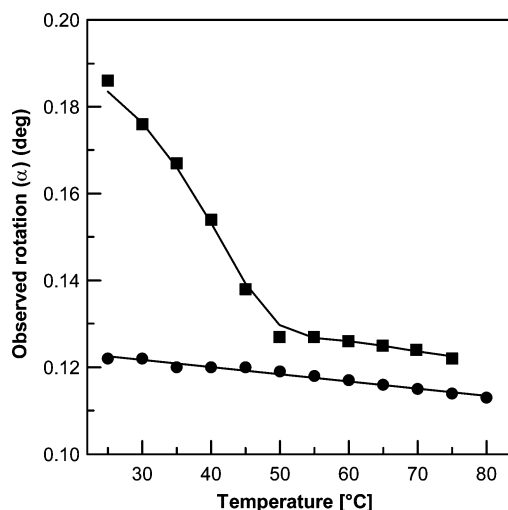
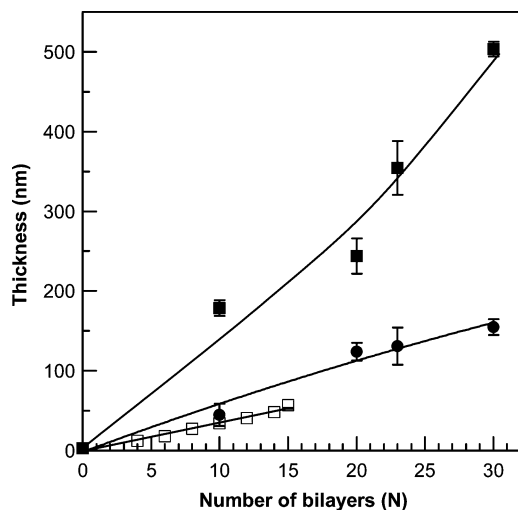


**Figure 3.** Dependence of rotation ( $\alpha$ ) of  $\lambda$ -carrageenan (circles) and  $\iota$ -carrageenan (squares) solutions ( $3 \text{ g}\cdot\text{L}^{-1}$  in 0.01 M KCl, pH 7) vs temperature measured by polarimetry. The lines are drawn as guides for the eye.

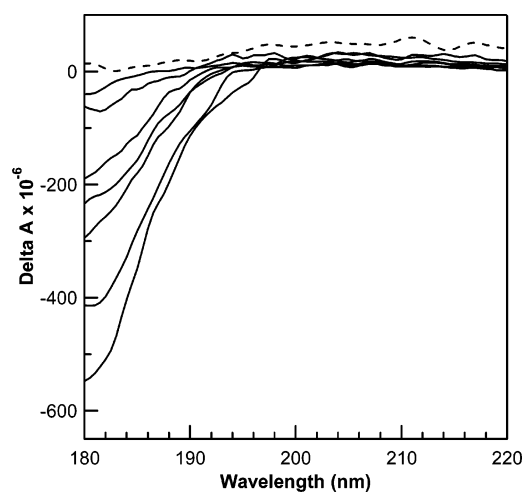
ecules adopt a random coil conformation in solution at room temperature, whereas  $\iota$ -carrageenan macromolecules are structured in helical conformation as expected.<sup>22,24–29</sup> The inspection of the variation of the observed rotation ( $\alpha$ ) as a function of the temperature (Figure 3) reveals a distinct behavior between both carrageenans: Whereas the  $\iota$ -carrageenan solution exhibits a marked decrease of  $\alpha$  with temperature increasing to  $50^\circ\text{C}$ , no significant variation was recorded for the  $\lambda$ -carrageenan solution. These results confirm that  $\lambda$ -carrageenan adopts a random coil conformation at any temperature and  $\iota$ -carrageenan shows a helix–coil transition upon increase of temperature as described before.<sup>22,34</sup> CD analyses were also performed on carrageenan solutions at pH 10 at room temperature (results not shown). No significant difference with the spectra measured at neutral pH was noticed, which indicates that the pH does not influence the conformation of these strongly charged polysaccharides under the conditions used.

Figure 4 shows the growth of PAH/carrageenan assemblies built up at pH 10. The growth of (PAH/ $\iota$ -carr) film built up at pH 7 was added for the comparison. In all the cases, a regular film growth was observed. However, films of higher thicknesses are obtained at pH 10 due to the lower degree of ionization of





**Figure 4.** Variation of the thickness of (PAH/ $\lambda$ -carr) grown at pH 10 (filled circles), (PAH/ $\iota$ -carr) grown at pH 10 (filled squares) and (PAH/ $\iota$ -carr) grown at pH 7 (opened squares) as a function of the number of deposited bilayers ( $N$ ) measured by ellipsometry in dried state. The lines are drawn as guides for the eye.



**Figure 5.** Circular dichroism spectra of (PAH/ $\lambda$ -carr)<sub>30</sub> (dashed line) and (PAH/ $\iota$ -carr) <sub>$N$</sub>  (continuous lines) films measured at room temperature in dried state. From top to bottom:  $N = 5, 8, 11, 13, 15, 23, 30$ .

the weak polycation PAH at this pH, as previously shown for other multilayer systems.<sup>47,48</sup> Therefore, in the sequel, we will report only on films grown at pH 10. In such conditions, the films prepared with  $\iota$ -carrageenan appear thicker than the ones based on  $\lambda$ -carrageenan. These films should be considered as molecular blends of PAH and carrageenans with profuse interpenetration of successive layers, as generally reported for LbL multilayers.<sup>49</sup>

Moreover CD measurements performed on (PAH/ $\lambda$ -carr) <sub>$N$</sub>  and (PAH/ $\iota$ -carr) <sub>$N$</sub>  films (Figure 5) reveal spectra similar to the ones measured for  $\lambda$ - and  $\iota$ -carrageenan solutions: Whereas no band is detected for nonoptically active films containing  $\lambda$ -carrageenan, a marked negative band is observed at 180 nm for  $\iota$ -carrageenan-based films. This good agreement between the CD spectra of carrageenan solutions and the multilayers proves that the conformations of the polysaccharides are essentially kept during the adsorption process. Furthermore, the CD spectra of (PAH/ $\iota$ -carr) <sub>$N$</sub>  multilayers of increasing thickness clearly show that the higher the number of deposited bilayers, the higher the intensity of the 180 nm band. Therefrom, we can conclude that  $\iota$ -carrageenan chains embedded into the film keep their struc-

tured helical conformation over the whole film thickness. However, since the CD spectra could not be measured below 180 nm, it was not possible to quantify the concentration in helices of our films. This behavior is in agreement with previous studies performed on gel complexes obtained by mixing chitosan and  $\iota$ -carrageenan solutions and for which it was shown that the helical conformation of  $\iota$ -carrageenan is preserved during the complex formation.<sup>50</sup> In the same way, biomacromolecules such as polypeptides,<sup>51–54</sup> DNA,<sup>55</sup> or proteins<sup>56</sup> were also shown to keep their secondary structure in multilayer films.

It was reported previously that the charge density of lowly charged polyelectrolytes can strongly influence the thickness of LbL films.<sup>57–59</sup> However, for more charged polyelectrolytes, it was shown that the thickness increment is independent of the linear charge density.<sup>57</sup> The  $\lambda$ - and  $\iota$ -carrageenans, which both contain from 1 to 1.5 sulfate group per saccharide unit, are highly charged polyelectrolytes. As a consequence, the difference in charge density between both polysaccharides is not the reason for the large difference in the thickness observed between both films. This variation should thus be ascribed to the different conformations adopted by  $\iota$ - and  $\lambda$ -carrageenan within the films. Indeed,  $\iota$ -carrageenan is adsorbed onto the surface in a structured helical conformation which is preserved during the multilayer buildup. The incorporation of such structured chains with a higher cross section results in films of higher thicknesses. Furthermore, circular dichroism measurements performed on heated (PAH/ $\iota$ -carr) multilayer films (results not shown) revealed that the helix–coil transition of  $\iota$ -carrageenan chains embedded within the film does not take place upon heating, even to temperature as high as 80 °C, contrasting with the behavior observed in aqueous solution.<sup>22,34</sup> In fact, the numerous electrostatic interactions between oppositely charged polyelectrolytes contribute to strongly reduce the motion of  $\iota$ -carrageenan chains in the multilayer, preventing any conformational change.

We investigated the influence of the polysaccharide conformation on the multilayer morphology by performing AFM imaging measurements on 30-bilayer samples ended by a carrageenan layer. Measurements were carried out at room temperature both on dried films and on films immersed in aqueous solution adjusted to pH 10. The inspection of the AFM images acquired in dried and wet states (Figure 6) reveals the presence of continuous films with very different morphologies depending on the carrageenan used. The multilayer based on  $\lambda$ -carrageenan presents a fuzzy surface with a high roughness (Table 1), and some valleys almost going down to the substrate. In contrast, the sample based on  $\iota$ -carrageenan appears flat with a low roughness (Table 1). In addition, we observed different behaviors between both films upon hydration. Whereas the  $\iota$ -carrageenan-based multilayer exhibits an increase of the external roughness, a slight decrease is seen for the  $\lambda$ -carrageenan-based film (Table 1). The inspection of the AFM images recorded in aqueous solution also reveals an increase in the lateral size of the aggregates present on the surface. This feature is more visible in the case of the (PAH/ $\lambda$ -carr)<sub>30</sub> sample. The different surface morphologies can be explained by considering the different conformations adopted by the polysaccharide chains. The adsorption of the flexible unstructured  $\lambda$ -carrageenan chains onto the multilayers results in the formation of rough multilayers, as frequently encountered when working with weakly charged polyelectrolytes such as PAH at pH 10.<sup>60</sup> In contrast, the adsorption of stiff helices of  $\iota$ -carrageenan leads to the formation of a flat and well-defined surface. The reorganization of polyelectrolyte chains upon hydration induces a slight smoothing of the soft external surface of (PAH/ $\lambda$ -carr)<sub>30</sub>

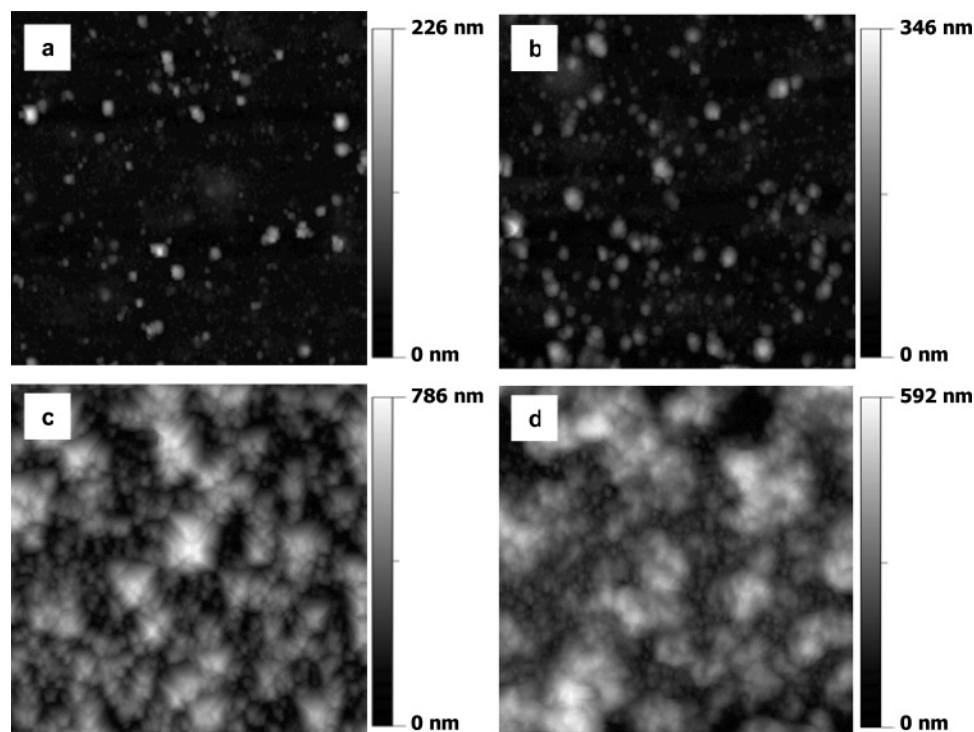


**Figure 6.**  $8 \times 8 \mu\text{m}^2$  topographic AFM images of (PAH/ $\iota$ -carr) $_{30}$  (a and b) and (PAH/ $\lambda$ -carr) $_{30}$  (c and d) films measured in air (left side) and in aqueous solution adjusted to pH 10 (right side).

**Table 1.** Average RMS Roughness of (PAH/ $\iota$ -carr) $_{30}$  and (PAH/ $\lambda$ -carr) $_{30}$  Films Measured by AFM in Air and in Aqueous Solution (pH 10) for Two Different Surface Areas

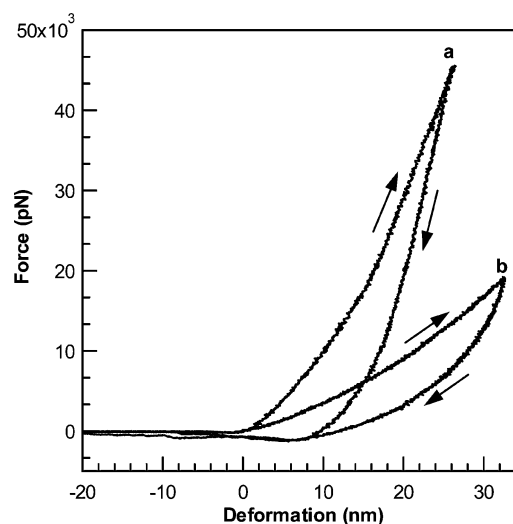
sample	surface area	average rms roughness <sup>a</sup> [nm]	
		dry state <sup>b</sup>	pH 10 <sup>b</sup>
(PAH/ $\iota$ -carr) $_{30}$	$8 \times 8 \mu\text{m}^2$	17 (1)	32 (6)
	$4 \times 4 \mu\text{m}^2$	16 (1)	29 (6)
(PAH/ $\lambda$ -carr) $_{30}$	$8 \times 8 \mu\text{m}^2$	148 (14)	114 (25)
	$4 \times 4 \mu\text{m}^2$	125 (16)	93 (15)

<sup>a</sup> The rms roughness value is an average of five measurements. <sup>b</sup> The number in parentheses is the standard deviation.

film.<sup>61</sup> In contrast, in the case of the (PAH/ $\iota$ -carr) $_{30}$  ended by stiff macromolecular helices, the hydration leads to an increase of the roughness.

Considering the strong difference in the characteristics of the films based on  $\iota$ - and  $\lambda$ -carrageenan, we investigated their mechanical properties by applying a deformation with an AFM tip used as a microindenter. All the measurements were performed in aqueous solution at pH 10 on carrageenan-ended films. Figure 7 displays the approach and withdrawal contact curves measured in a selected area of 30-bilayer samples prepared with  $\iota$ -carrageenan and  $\lambda$ -carrageenan, respectively. The inspection of these curves reveals different features: First, the self-assembly based on  $\iota$ -carrageenan appears significantly stiffer than the one based on  $\lambda$ -carrageenan, since a higher force is required to achieve the same sample deformation. Furthermore, a nonoverlapping of the approach and withdrawal curves is observed both for (PAH/ $\lambda$ -carr) $_{30}$  and (PAH/ $\iota$ -carr) $_{30}$  films. This hysteresis points out an elastoplastic behavior.<sup>62</sup> However, frequency vs force measurements revealed no significant difference (results not shown) indicating no viscoelasticity on a time scale of the AFM technique.

The use of the Hertz model which assumes an infinite sample thickness is very common to estimate the Young's modulus ( $E$ ) of elastic material from the force vs deformation experiments.<sup>63,64</sup> However, when the material is a thin film deposited

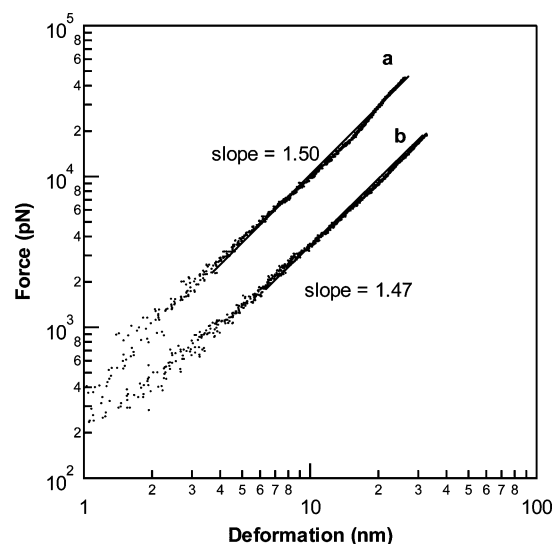


**Figure 7.** Force vs deformation curves measured by AFM in aqueous solution (pH 10): (a) (PAH/ $\iota$ -carr) $_{30}$  and (b) (PAH/ $\lambda$ -carr) $_{30}$  films. The arrows indicate the approach and withdrawal curves for each sample.

onto a hard substrate, several studies have pointed out the need to take the thickness of the film in the model into account.<sup>14,65–68</sup> The thicknesses of our films measured in aqueous solution by AFM by scratching off a part of the multilayer were 800 and 300 nm for (PAH/ $\iota$ -carr) $_{30}$  and (PAH/ $\lambda$ -carr) $_{30}$ , respectively. This corresponds, for both cases, to a swelling by a factor 2 in aqueous solution. As a consequence, the maximal indentation depth applied during the force vs distance measurements did not exceed 10% of the film thickness, which corresponds to the small deformation regime. Under these conditions, we expect that the thickness of the sample has only a weak influence on the determination of the Young's modulus. To check this assumption, we compared the Young's modulus values extracted by four different models: the Hertz model, which does not take the influence of the thickness of the sample into account,<sup>45</sup> and three other thickness-corrected models, namely, Makushkin,<sup>66</sup>

**Table 2.** Young's Modulus Values Estimated from Force vs Deformation Curves for (PAH/*l*-carr)<sub>30</sub> and (PAH/*λ*-carr)<sub>30</sub> Films Immersed in Aqueous Solution (pH 10) According to Different Mathematical Models

mathematical model	Young's modulus [MPa]	
	(PAH/ <i>l</i> -carr) <sub>30</sub>	(PAH/ <i>λ</i> -carr) <sub>30</sub>
Hertz	32 ± 3	10 ± 2
Makushkin	31 ± 3	9 ± 1
Akhremitchev	29 ± 3	7 ± 1
Dimitriadis	26 ± 3	7 ± 1

**Figure 8.** Force vs deformation log-log profiles measured in approach for (a) (PAH/*l*-carr)<sub>30</sub> and (b) (PAH/*λ*-carr)<sub>30</sub> films immersed in aqueous solution (pH 10). The lines are fit to the data.

Akhremitchev,<sup>65</sup> and Dimitriadis.<sup>68</sup> The Young's modulus values calculated from these different models are presented in Table 2 for (PAH/*λ*-carr)<sub>30</sub> and (PAH/*l*-carr)<sub>30</sub> films. Only small differences are noticed between the values, showing that the consideration of the thickness of the films is not crucial for the determination of Young's modulus from the models. Therefore, we systematically used the Hertz model to analyze our data in the sequel

$$F = \frac{4}{3(1 - \nu^2)} \times ER^{1/2}\delta^{3/2} \quad (2)$$

Figure 8 displays the log-log profile of force-deformation curves measured in approach for (PAH/*λ*-carr)<sub>30</sub> and (PAH/*l*-carr)<sub>30</sub> films. The experimental data are correctly fitted by linear curves with a slope of about 1.5 which is in good agreement with the Hertz model. To get reliable results, we performed similar force vs deformation measurements in 40 different areas of the samples. The average Young's moduli extracted from these samplings and determined according to the Hertz model (eq 2) are 35 ± 5 MPa and 7.5 ± 2 MPa for films prepared with *l*-carrageenan and *λ*-carrageenan, respectively. The values of the Young's modulus determined previously by others were between several 100 MPa for very stiff multilayers based on poly(styrene sulfonate) (PSS) and PAH<sup>69</sup> and ~20 kPa for very soft films such as poly(L-lysine) (PLL)/hyaluronic acid (HA) assemblies.<sup>14</sup> By considering this range of modulus values, we can conclude that our films are relatively soft materials typical for an elastomeric material. Moreover, the higher stiffness and the higher value of Young's modulus measured for (PAH/*l*-carr) films are explained by the presence of structured helices

which contribute to reinforcing the mechanical properties of the assembly. Similar differences in mechanical behavior were previously evidenced by performing rheological measurements on complex gels prepared by mixing chitosan and *l*- or *λ*-carrageenan solutions;<sup>50</sup> it was suggested that additional cross-links due to the presence of double helices of *l*-carrageenan-based complex may contribute to strongly reinforcing the strength of the gel, although this point is still debated.<sup>30–32</sup>

## Conclusion

In this study, we showed the formation of polyelectrolyte films based on a synthetic polycation, PAH, and two different polysaccharides, *l*- and *λ*-carrageenans, which mainly differ by their conformation. The inspection of the morphology and the internal structure of the films clearly reveals that the helical conformation adopted by *l*-carrageenan in solution is kept during the multilayer buildup. The presence of such ordered structures results in films with a higher thickness and a higher Young's modulus compared to the unstructured *λ*-carrageenan-based ones. Therefore, we provide the evidence that the characteristics and mechanical properties of multilayers strongly depend on the conformation of the polyelectrolyte chains used to prepare the films. The approach consisting of varying the structure of polyelectrolytes used during the LbL process should open a new way to prepare coatings showing a gradient of mechanical properties over the nanometer scale.

**Acknowledgment.** Dr. P. Cosette (Rouen University) is thanked for his help with circular dichroism measurements. Dr. M. Grisel (Le Havre University) is acknowledged for providing access to the polarimeter. Brunero Capella is thanked for his helpful discussions about force measurements onto polymeric materials. The research was financially supported by the French-German network "Complex Fluids : From 3D to 2D" and by the European INTERREG IIIA program (AMACOM project).

## References and Notes

- (1) Decher, G.; Hong, J. D.; Schmitt, J. *Thin Solid Films* **1992**, *210*, 831.
- (2) Decher, G. *Science* **1997**, *277*, 1232.
- (3) Bertrand, P.; Jonas, A. M.; Laschewsky, A.; Legras, R. *Macromol. Rapid Commun.* **2000**, *21*, 319.
- (4) Arys, X.; Jonas, A. M.; Laschewsky, A.; Legras, R. In *Supramolecular Polymers*; Cifferi, A., Ed.; Marcel Dekker, New York, 2000; p 505.
- (5) Jiang, X. P.; Hammond, P. T. *Langmuir* **2000**, *16*, 8501.
- (6) Clark, S. L.; Montague, M.; Hammond, P. T. *Supramol. Sci.* **1997**, *4*, 141.
- (7) Pallandre, A.; Glinel, K.; Jonas, A. M.; Nysten, B. *Nano Lett.* **2004**, *4*, 365.
- (8) Pallandre, A.; Moussa, A.; Nysten, B.; Jonas, A. M. *Adv. Mater.* In press.
- (9) *Multilayer Thin Films: Sequential Assembly of Nanocomposite Materials*; Decher, G.; Schlenoff, J. B., Eds.; Wiley-VCH: Weinheim, 2003.
- (10) Hammond, P. T. *Curr. Opin. Colloid Interface Sci.* **1999**, *4*, 430.
- (11) Hiller, J.; Mendelsohn, J. D.; Rubner, M. F. *Nat. Mater.* **2002**, *1*, 59.
- (12) Rmaile, H. H.; Schlenoff, J. B. *J. Am. Chem. Soc.* **2003**, *125*, 6602.
- (13) Peyratout, C. S.; Daehne, L. *Angew. Chem., Int. Ed.* **2004**, *43*, 3762.
- (14) Richert, L.; Engler, A. J.; Discher, D. E.; Picart, C. *Biomacromolecules* **2004**, *5*, 1908.
- (15) Richert, L.; Boulmedais, F.; Laval, P.; Mutterer, J.; Ferreux, E.; Decher, G.; Schaaf, P.; Voegel, J.-C.; Picart, C. *Biomacromolecules* **2004**, *5*, 284.
- (16) Schneider, A.; Francius, G.; Obeid, R.; Schwinté, P.; Hemmerle, J.; Frisch, B.; Schaaf, P.; Voegel, J.-C.; Senger, B.; Picart, C. *Langmuir* **2006**, *22*, 1193.

- (17) Mermut, O.; Lefebvre, J.; Gray, D. G.; Barrett, C. J. *Macromolecules* **2003**, *36*, 8819.
- (18) Tang, Z.; Kotov, N. A.; Magonov, S.; Ozturk, B. *Nat. Mater.* **2003**, *2*, 413.
- (19) Mamedov, A. A.; Kotov, N. A.; Prato, M.; Guldi, D. M.; Wicksted, J. P.; Hirsch, A. *Nat. Mater.* **2002**, *1*, 257.
- (20) De Ruiter, G. A.; Rudolph, B. *Trends Food Sci. Technol.* **1997**, *8*, 389.
- (21) Therkelsen, G. H. In *Industrial Gums — Polysaccharides and Their Derivatives*, 3rd ed.; Whistler, R. L., BeMiller, J. N., Eds.; Academic Press: New York, 1993; Chapter 7.
- (22) van de Velde, F.; De Ruiter, G. A. In *Biopolymers — Polysaccharides II*; Vandamme, E. J., De Baets, S., Steinbüchel, A., Eds.; Wiley-VCH Verlag GmbH: Weinheim, 2002; Chapter 9.
- (23) The well-studied  $\kappa$ -carrageenan was not selected due to its high ability to form large aggregates and gels.
- (24) Bongaerts, K.; Paoletti, S.; Deneff, B.; Vanneste, K.; Cuppo, F.; Reynaers, H. *Macromolecules* **2000**, *33*, 8709.
- (25) Reynaers, H. *Fibres Text. East Eur.* **2003**, *11*, 88.
- (26) Hugerth, A.; Caram-Lelham, N.; Sundelöf, L.-O. *Carbohydr. Polym.* **1997**, *34*, 149.
- (27) Balcerski, J. S.; Pysh, E. S.; Chen, G. C.; Yang, J. T. *J. Am. Chem. Soc.* **1975**, *97*, 6274.
- (28) Arndt, E. R.; Stevens, E. S. *Carbohydr. Res.* **1997**, *303*, 73.
- (29) Janaswamy, S.; Chandrasekaran, R. *Carbohydr. Res.* **2002**, *337*, 523.
- (30) Smidsrod, O.; Andresen, I. L.; Grasdalen, H.; Larsen, B.; Painter, T. *Carbohydr. Res.* **1980**, *80*, C11.
- (31) Anderson, N. S.; Campbell, J. W.; Harding, M. M.; Rees, D. A.; Samuel, J. W. *J. Mol. Biol.* **1969**, *45*, 85.
- (32) Viebke, C.; Borgstroem, J.; Piculell, L. *Carbohydr. Polym.* **1995**, *27*, 145.
- (33) Vanneste, K.; Sloomackers, D.; Reynaers, H. *Food Hydrocolloids* **1996**, *10*, 99.
- (34) Hossain, K. S.; Miyahara, K.; Maeda, H.; Nemoto, N. *Biomacromolecules* **2001**, *2*, 442.
- (35) Grinberg, V. Y.; Grinberg, N. V.; Usov, A. I.; Shusharina, N. P.; Khoklov, A. R.; de Kruif, K. G. *Biomacromolecules* **2001**, *2*, 864.
- (36) Glinel, K.; Sukhorukov, G. B.; Möhwald, H.; Khrenov, V.; Tauer, K. *Macromol. Chem. Phys.* **2003**, *204*, 1784.
- (37) Quinn, J. F.; Caruso, F. *Langmuir* **2004**, *20*, 20.
- (38) Van Landingham, M. R. *Microsc. Today* **1997**, *97*, 12.
- (39) Hutter, J. L.; Bechhoefer, J. *Rev. Sci. Instrum.* **1993**, *64*, 1868.
- (40) J. E. Sader, J. E.; Larson, I.; Mulvaney, P.; White, L. R. *Rev. Sci. Instrum.* **1995**, *66*, 3789.
- (41) Butt, H.-J.; Capella, B.; Kappl, M. *Surf. Sci. Rep.* **2005**, *59*, 1.
- (42) Cant, N. E.; Critchley, K.; Zhang, H.-L.; Evans, S. D. *Thin Solid Films* **2003**, *426*, 31.
- (43) Villarrubia, J. S. *Surf. Sci.* **1994**, *321*, 287.
- (44) Information about PUNIAS program can be found on the following website: <http://site.voila.fr/punias>.
- (45) Timoshenko, S. P.; Goodier, N. N. *Theory of Elasticity*, 2nd ed.; McGraw-Hill Book Co.: New York, 1951.
- (46) Mueller, R.; Kohler, K.; Weinkamer, R.; Sukhorukov, G. B.; Fery, A. *Macromolecules* **2005**, *38*, 9766.
- (47) Shiratori, S. S.; Rubner, M. F. *Macromolecules* **2000**, *33*, 4213.
- (48) Park, S. Y.; Rubner, M. F.; Mayes, A. M. *Langmuir* **2002**, *18*, 9600.
- (49) Glinel, K.; Jonas, A. M.; Laschewsky, A.; Vuillaume, P. In *Multilayer Thin Films: Sequential Assembly of Nanocomposite Materials*; Decher, G., Schlenoff, J. B., Eds.; Wiley-VCH: Weinheim, 2003; Chapter 7, p 177.
- (50) Shumilina, E. V.; Shchipunov, Y. U. *Colloid J.* **2002**, *64*, 372.
- (51) Zhi, Z.-L.; Haynie, D. T. *Macromolecules* **2004**, *37*, 8668.
- (52) Müller, M. *Biomacromolecules* **2001**, *2*, 262.
- (53) Boulmedais, F.; Bozonnet, M.; Schwinté, P.; Voegel, J.-C.; Schaaf, P. *Langmuir* **2003**, *19*, 9873.
- (54) Haynie, D. T.; Zhang, L.; Rudra, J. S.; Zhao, W.; Zhong, Y.; Palath, N. *Biomacromolecules* **2005**, *6*, 2895.
- (55) Montrel, M. M.; Sukhorukov, G. B.; Petrov, A. I.; Shabarchina, L. I.; Sukhorukov, B. I. *Sens. Actuators, B* **1997**, *42*, 225.
- (56) Schwinté, P.; Voegel, J.-C.; Picart, C.; Haikel, Y.; Schaaf, P.; Szalontai, B. *J. Phys. Chem. B* **2001**, *105*, 11906.
- (57) Glinel, K.; Moussa, A.; Jonas, A. M.; Laschewsky, A. *Langmuir* **2002**, *18*, 1408.
- (58) Steitz, R.; Jaeger, W.; von Klitzing, R. *Langmuir* **2001**, *17*, 4471.
- (59) Schoeler, B.; Kumaraswamy, G.; Caruso, F. *Macromolecules* **2002**, *35*, 889.
- (60) Menchaca, J.-L.; Jachimska, B.; Cuisinier, F.; Perez, E. *Colloids Surf., A* **2003**, *222*, 185.
- (61) Kugler, R.; Schmitt, J.; Knoll, W. *Macromol. Chem. Phys.* **2002**, *203*, 413.
- (62) Capella, B.; Kaliappan, S. K.; Sturm, H. *Macromolecules* **2005**, *38*, 1874.
- (63) Domke, J.; Radmacher, M. *Langmuir* **1998**, *14*, 3320.
- (64) Uricanu, V. I.; Duits, M. H. G.; Mellema, J. *Langmuir* **2004**, *20*, 5079.
- (65) Akhremitchev, B. B.; Walker, G. C. *Langmuir* **1999**, *15*, 5630.
- (66) Lancaster, J. K. *J. Phys. D* **1982**, *15*, 1125.
- (67) Chizhik, S. A.; Huang, Z.; Gorbunov, V. V.; Myshkin, N. K.; Tsukruk, V. V. *Langmuir* **1998**, *14*, 2606.
- (68) Dimitriadis, E. K.; Horkay, F.; Maresca, J.; Kachar, B.; Chadwick, R. S. *Biophys. J.* **2002**, *82*, 2798.
- (69) Heuvingh, J.; Zappa, M.; Fery, A. *Langmuir* **2005**, *21*, 3165.

BM060378A